Journal of Pathology
J Pathol 2021
Published online 16 November 2021 in Wiley Online Library (wileyonlinelibrary.com) DOI: 10.1002/path.5814

ORIGINAL PAPER

RAF1–MEK/ERK pathway-dependent ARL4C expression promotes ameloblastoma cell proliferation and osteoclast formation

Shinsuke Fujii[1*], Takuma Ishibashi[1†], Megumi Kokura[1†], Tatsufumi Fujimoto[1], Shinji Matsumoto[2,3], Satsuki Shidara[1‡], Kari J Kurppa[4], Judith Pape[5], Javier Caton[6], Peter R Morgan[7], Kristiina Heikinheimo[8], Akira Kikuchi[2], Eijiro Jimi[9,10] and Tamotsu Kiyoshima[1]

[1] *Laboratory of Oral Pathology, Division of Maxillofacial Diagnostic and Surgical Sciences, Faculty of Dental Science, Kyushu University, Fukuoka, Japan*
[2] *Department of Molecular Biology and Biochemistry, Graduate School of Medicine, Osaka University, Suita, Japan*
[3] *Integrated Frontier Research for Medical Science Division, Institute for Open and Transdisciplinary Research Initiatives (OTRI), Osaka University, Suita, Japan*
[4] *Institute of Biomedicine and MediCity Research Laboratories, University of Turku, and Turku Bioscience Centre, University of Turku and Åbo Akademi University, Turku, Finland*
[5] *Division of Surgery and Interventional Science, Department of Targeted Intervention, Centre for 3D Models of Health and Disease, University College London, London, UK*
[6] *Department of Anatomy and Embryology, Faculty of Medicine, University Complutense Madrid, Madrid, Spain*
[7] *Head & Neck Pathology, King's College London, Guy's Hospital, London, UK*
[8] *Department of Oral and Maxillofacial Surgery, Institute of Dentistry, University of Turku and Turku University Hospital, Turku, Finland*
[9] *Oral Health/Brain Health/Total Health Research Center, Faculty of Dental Science, Kyushu University, Fukuoka, Japan*
[10] *Laboratory of Molecular and Cellular Biochemistry, Faculty of Dental Science, Kyushu University, Fukuoka, Japan*

**Correspondence to: S Fujii, Laboratory of Oral Pathology, Division of Maxillofacial Diagnostic and Surgical Sciences, Faculty of Dental Science, Kyushu University, 3-1-1 Maidashi, Higashi-ku, Fukuoka 812-8582, Japan. E-mail: sfujii@dent.kyushu-u.ac.jp*

[†]These authors contributed equally to this work as second authors.
[‡]Present address: Department of Orthodontics, Tokyo Dental College, 1-2-2 Masago, Mihamaku, Chiba261-8502, Japan

Abstract

Ameloblastoma is an odontogenic neoplasm characterized by slow intraosseous growth with progressive jaw resorption. Recent reports have revealed that ameloblastoma harbours an oncogenic *BRAF*V600E mutation with mitogen-activated protein kinase (MAPK) pathway activation and described cases of ameloblastoma harbouring a *BRAF*V600E mutation in which patients were successfully treated with a BRAF inhibitor. Therefore, the MAPK pathway may be involved in the development of ameloblastoma; however, the precise mechanism by which it induces ameloblastoma is unclear. The expression of ADP-ribosylation factor (ARF)-like 4c (ARL4C), induced by a combination of the EGF–MAPK pathway and Wnt/β-catenin signalling, has been shown to induce epithelial morphogenesis. It was also reported that the overexpression of ARL4C, due to alterations in the EGF/RAS–MAPK pathway and Wnt/β-catenin signalling, promotes tumourigenesis. However, the roles of ARL4C in ameloblastoma are unknown. We investigated the involvement of ARL4C in the development of ameloblastoma. In immunohistochemical analyses of tissue specimens obtained from 38 ameloblastoma patients, ARL4C was hardly detected in non-tumour regions but tumours frequently showed strong expression of ARL4C, along with the expression of both BRAFV600E and RAF1 (also known as C-RAF). Loss-of-function experiments using inhibitors or siRNAs revealed that ARL4C elevation depended on the RAF1–MEK/ERK pathway in ameloblastoma cells. It was also shown that the RAF1–ARL4C and BRAFV600E–MEK/ERK pathways promoted cell proliferation independently. ARL4C-depleted tumour cells (generated by knockdown or knockout) exhibited decreased proliferation and migration capabilities. Finally, when ameloblastoma cells were co-cultured with mouse bone marrow cells and primary osteoblasts, ameloblastoma cells induced osteoclast formation. ARL4C elevation in ameloblastoma further promoted its formation capabilities through the increased RANKL expression of mouse bone marrow cells and/or primary osteoblasts. These results suggest that the RAF1–MEK/ERK–ARL4C axis, which may function in cooperation with the BRAFV600E–MEK/ERK pathway, promotes ameloblastoma development.

Keywords: ameloblastoma; ARL4C; BRAFV600E; RAF1; proliferation; osteoclast formation

Received 19 April 2021; Revised 10 September 2021; Accepted 5 October 2021

No conflicts of interest were declared.

Introduction

Ameloblastoma, which originates from the dental lamina, is classified as a benign epithelial odontogenic tumour, showing slow intraosseous growth with progressive bone resorption of the jaw [1]. Ameloblastoma is the most common odontogenic tumour, excluding odontomas, tending to recur locally if not adequately removed. Clinically, with increased size, complications include loosening of teeth, malocclusion, paraesthesia, pain, limited mouth opening, difficult mastication, and airway obstruction [1]. The main treatment is wide surgical resection with an area of bone beyond radiographic margins; this necessarily results in facial deformity [2]. Ameloblastomas are classified as ameloblastoma (also called conventional ameloblastoma or solid/multicystic ameloblastoma), unicystic ameloblastoma, extraosseous/peripheral ameloblastoma, and metastasizing ameloblastoma. Unicystic ameloblastoma is further classified into luminal, intraluminal, and mural subtypes [3]. The common histopathological patterns of ameloblastoma are follicular and plexiform [1]. The definitive underlying pathogenic mechanisms of ameloblastoma, including an increase in ameloblastoma cells and enhanced bone resorption capabilities through osteoclast formation, remain unclear. Therefore, a novel tumour therapy based on the molecular mechanisms underlying ameloblastoma development is awaited.

In the age of precision cancer medicine, tumour specimens are processed for next-generation sequencing with gene panel tests to detect gene mutations/variants for optimizing therapeutic intervention [4]. As ameloblastomas are rare, with an incidence of 0.5 cases per million population [1,5], information concerning the molecular mechanisms involved in the aetiology of ameloblastoma is limited. It is thus necessary to investigate the roles of individual signal transduction in relation to the aetiology using pathological specimens or cell lines.

A *BRAF* mutation, causing valine to glutamic acid substitution at codon 600 (V600E), is present in 40–60% of ameloblastoma cases with mutation-dependent mitogen-activated protein kinase (MAPK) pathway activation [6–9]. Several studies have described cases of patients with a *BRAF*V600E mutant that were successfully treated with BRAF inhibitors [10–12], suggesting that *BRAF*V600E signalling might be involved in the development of ameloblastoma. However, the details of the MAPK pathway-dependent mechanism through which ameloblastoma develops are poorly understood.

ADP-ribosylation factor (ARF)-like proteins (ARLs) are a subgroup of the ARF small GTP-binding protein superfamily [13]. Recent studies have shown that ARL4C, a member of ARL family proteins, is a target molecule induced by activation of the RAS–MAPK pathway and Wnt/β-catenin signalling and it plays an important role in both epithelial morphogenesis and tumourigenesis [14–18]. For instance, ARL4C is expressed in some epithelial rudiments, including tooth buds, hair follicles, salivary glands, and kidneys of E15 mouse embryos [14]. The particularly high expression of ARL4C in the distal tip of ureteric buds (UBs) of the mouse embryonic kidney, due to the FGF–RAS–MAPK pathway and Wnt/β-catenin signalling activation, was shown to be involved in UB branching morphogenesis [14].

In contrast, the effects of ARL4C on epithelial tooth bud morphogenesis, which has the same origin as ameloblastoma, remain unclear. ARL4C expression is also upregulated in cancers and is associated with the progression of tumourigenesis, including colorectal, lung, tongue, liver, gastric, renal cell, ovarian cancers, and glioblastoma [15–17,19–22]. ARL4C expression was reportedly induced in lung premalignant lesions and the exogenous expression of ARL4C promoted cell proliferation of human immortalized small airway epithelial cells [18], indicating the proliferative capabilities of ARL4C, even in premalignant lesions. However, neither ARL4C expression in ameloblastoma nor the effects of its signalling on ameloblastoma development are well understood.

In this study, we found elevated expression of ARL4C in ameloblastoma cell lines and pathological specimens and demonstrated the role of ARL4C in regulating ameloblastoma cellular growth and ameloblastoma-mediated osteoclast formation.

Materials and methods

Patients and immunohistochemistry

Human ameloblastoma ($n = 38$) tissues were obtained from patients who visited the Department of Oral and Maxillofacial Surgery, Kyushu University Hospital in the last 10 years (from December 2008 to September 2019), who were diagnosed with ameloblastoma or ameloblastoma, unicystic type according to the recent WHO Classification [1], and who underwent surgery. The clinicopathological data of the patients with ameloblastoma are presented in supplementary material, Table S1. The study protocol was approved by the ethics review board of the local ethics committee of Kyushu University, Japan (#29-392). Resected specimens were examined macroscopically to determine the location and size of ameloblastoma, and histological specimens were fixed in 10% (v/v) formalin and processed for paraffin embedding. Specimens were sectioned (thickness 4 μm) and stained with haematoxylin and eosin (H&E) for independent evaluation by three pathologists.

Immunohistochemical staining was performed as described previously [23,24]. Further details are provided in Supplementary materials and methods.

Cells and reagents

AM-1 human ameloblastoma cells were kindly provided by Dr H Harada (Iwate Medical University, Shiwa-gun, Japan) [25]. AB10 and ABSV, primary ameloblastoma cells, HeLaS3 human uterine cancer cells, A549 human

lung adenocarcinoma cells, and NCI-H520 human lung squamous cell carcinoma cells were used in a previous study [6,15,16]. Lenti-X™ 293T (X293T) cells were purchased from Takara Bio Inc (Shiga, Japan). AM-1 cells were cultured in Keratinocyte SFM medium (Invitrogen, Carlsbad, CA, USA). AB10 and ABSV were cultured in CnT-PR medium (CELLnTEC, Bern, Switzerland). HeLaS3, A549, and X293T cells were grown in Dulbecco's modified Eagle's medium (Invitrogen) supplemented with 10% FBS (Invitrogen). NCI-H520 cells were grown in RPMI-1640 (Invitrogen) supplemented with 10% FBS. More details may be found in Supplementary materials and methods.

Plasmid construction and infection using lentivirus harbouring a cDNA

Lentiviral vectors were constructed by subcloning GFP, pEGFPN3-ARL4C, and ARF6^{Q67L} cDNAs into CSII-CMV-MCS-IRES2-Bsd (kindly provided by Dr H Miyoshi, RIKEN BioResource Center, Ibaraki, Japan) [14,26]. The vectors were then transfected with the packaging vectors, pCAG-HIV-gp and pCMV-VSV-G-RSV-Rev, into X293T cells using Lipofectamine LTX reagent (Invitrogen) to generate lentiviruses [27]. Further details are provided in Supplementary materials and methods.

Knockdown of protein expression by siRNA and quantitative RT-PCR

The effects of protein knockdown by siRNA were analysed as previously described [28]. In brief, siRNAs (final concentration 20 nM) were transfected into AM-1 cells using Lipofectamine RNAiMAX (Invitrogen). The target sequences are listed in supplementary material, Table S2. The transfected cells were then used for experiments conducted at 48 h post-transfection.

RT-qPCR was performed as described previously [29]. The primers used are listed in supplementary material, Table S3.

Generation of *ARL4C*-knockout cells

The target sequence for human *ARL4C*, 5'-CTTC TCGGTGTTGAAGCCGA-3', was designed with the help of CRISPR Genome Engineering Resources (https://zlab.bio/guide-design-resources) [30]. The plasmids, which were pX330 expressing hCas9, and single-guide RNA (sgRNA) targeting ARL4C and blasticidin resistance, were transfected into AM-1 cells using Lipofectamine LTX reagent, and the transfected cells were selected in medium containing 5 μg/ml blasticidin S (FUJIFILM Wako, Osaka, Japan) [16]. Single colonies were picked, mechanically disaggregated, and replated into individual wells of 24-well plates.

Osteoclast formation

Mouse primary osteoblasts (POBs) were obtained from the calvaria of newborn C57B16/J mice (The Jackson Laboratory, Bar Harbor, ME, USA) by a conventional method using collagenase, as described previously [31]. Mouse bone marrow cells (BMCs) (2×10^6 cells) were isolated from 6-week-old C57B16/J mice and co-cultured with the POBs (1×10^4 cells) in 0.225 ml of α-MEM containing 10% FBS and 0.075 ml of Keratinocyte SFM in 48-well plates. AM-1 cells (2×10^4 cells) were then added to the co-culture system. After 7 days, the cells were fixed and stained for tartrate-resistant acid phosphatase (TRAP). TRAP-positive cells were counted as osteoclast-like cells. The bone-resorbing activity of osteoclasts was assessed using an Osteo Assay Plate (Corning, Corning, NY, USA).

Statistical analysis

Statistical analyses were performed using JMP Pro 15 software (JMP, Marlow, UK). Significant differences were determined using Fisher's exact test for clinicopathological analyses. For other experiments, significant differences were determined using Student's *t*-test and one-way ANOVA with Tukey's test. $p < 0.05$ was considered to indicate statistical significance.

Additional assays

Cell proliferation and migration assays were performed as previously described [29,32]. Western blotting data were representative of at least three independent experiments.

Results

ARL4C is expressed in human ameloblastoma tissue

Immunohistochemical analyses were carried out to examine the expression of ARL4C in human ameloblastoma specimens. Clinicopathologically, no significant differences were observed between conventional and unicystic ameloblastomas, regarding sex, location, size, or recurrence (supplementary material, Table S1). Cytoplasmic staining for ARL4C was observed in 28 (73.7%) of 38 tumour cases, whereas it was hardly detected in adjacent oral non-tumourous stratified squamous cell regions, consistent with a previous report (Figure 1) [16]. The results were considered positive when more than 40% of the total epithelial cells within a single specimen were stained with anti-ARL4C antibody. Interestingly, ARL4C was strongly expressed in the tumour cells invading the surrounding stroma (Figure 1, black arrowheads). No association was found between ARL4C expression and location, sex, size, or recurrence (Table 1). The positive rates of ARL4C staining were lower in ameloblastoma, unicystic type (2/7; 28.6%) than in ameloblastoma (26/31; 74.3%) ($p < 0.01$; Fisher's exact test) (Figure 1), suggesting that the

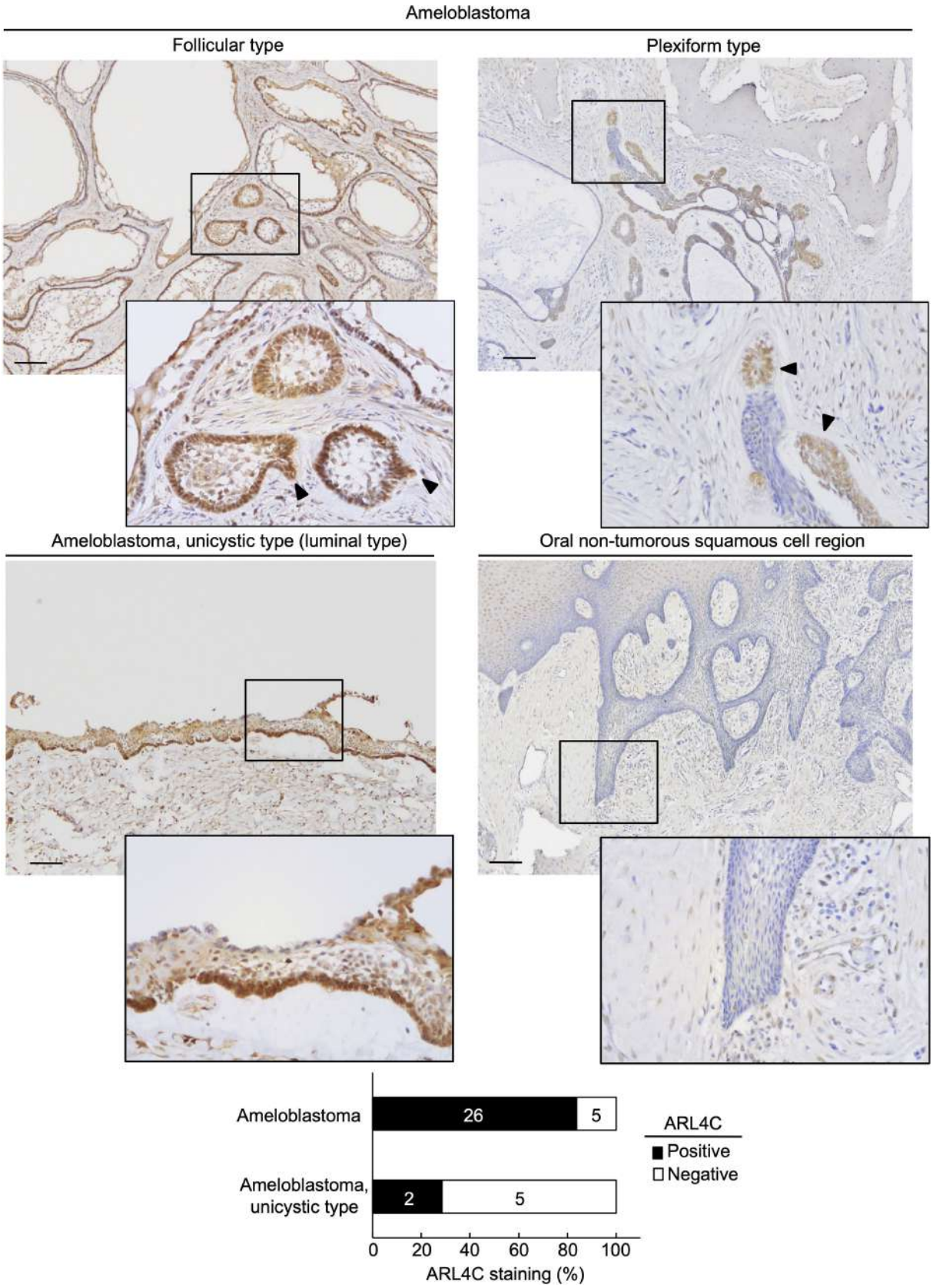

Figure 1. ARL4C is expressed in human ameloblastomas. Ameloblastoma tissues ($n = 38$) were stained with anti-ARL4C antibody and haematoxylin. Ameloblastoma and ameloblastoma, unicystic type were examined, and ARL4C-positive and -negative cases in each type are shown in the lower panel. Black boxes show enlarged images. Black arrowheads indicate ameloblastoma cells that invade the stroma. Scale bars: 100 μm.

Table 1. Clinical characteristics of ameloblastoma patients with ARL4C expression.

Categorical variables	ARL4C-positive ($n = 28$)	ARL4C-negative ($n = 10$)
Age	39.9 ± 16.7	34.9 ± 20.9
Location		
Mandible	22 (57.9%)	9 (23.7%)
Maxilla	6 (15.8%)	1 (2.6%)
Sex		
Male	18 (47.4%)	6 (15.8%)
Female	10 (26.3%)	4 (10.5%)
Size		
Mesiodistal ×	37.7 ± 18.5 ×	42.4 ± 17.9 ×
buccolingual ×	21.9 ± 9.2 ×	25.4 ± 7.7 ×
vertical (mm)	27.3 ± 13.5	51.7 ± 29.9
Clinical prognosis		
Primary	24 (63.2%)	6 (15.8%)
Recurrence	4 (10.5%)	4 (10.5%)

Size was calculated by computed tomography scan. Radiographically, image characteristics of ameloblastoma and ameloblastoma, unicystic type were multilocular and unilocular, respectively.

expression of ARL4C might be related to the ameloblastoma subtypes.

RAF1-dependent ARL4C expression is required for ameloblastoma cell proliferation

Since ARL4C is efficiently transcribed by the simultaneous activation of the RAS–MAPK pathway and Wnt/β-catenin signalling [14,15], we examined the molecular mechanism by which ARL4C expression is induced in ameloblastoma using AM-1 cells, an ameloblastoma cell line harbouring a *BRAF*V600E mutation [8]. ARL4C expression in AM-1 cells was comparable to that in A549, SAS, and NCI-H520 cells, wherein the elevated expression of ARL4C is involved in tumourigenesis [15,16] (Figure 2A). β-Catenin siRNA and PD168393 (a selective EGFR inhibitor) did not affect ARL4C expression, but the simultaneous inactivation of the EGFR pathway and β-catenin signalling reduced ARL4C (supplementary material, Figure S1A).

As *BRAF*V600E-dependent MAPK activation regulates ameloblastoma cell proliferation, we examined the effects of MAPK activation on ARL4C expression in AM-1 cells. The inhibition of the MAPK pathway by PD184161 (a selective MEK1/2 inhibitor) suppressed ERK1/2 activation and reduced ARL4C expression (Figure 2B), suggesting that ARL4C is dependent on MEK/ERK activation in AM-1 cells. Surprisingly, BRAFV600E inhibitors SB590885, dabrafenib, and vemurafenib reduced ERK activation but did not affect ARL4C expression (Figure 2B and supplementary material, Figure S1B). In addition, BRAF knockdown did not reduce ARL4C expression (Figure 2C and supplementary material, Figure S1C), suggesting that ARL4C might depend on another MEK/ERK pathway, besides the BRAFV600E-dependent MEK/ERK pathway, in AM-1 cells.

BRAF reportedly forms a complex with wild-type RAF1 (also known as C-RAF) and then increases RAF1 kinase activity, thereby stimulating the MEK/ERK pathway [33,34]. Therefore, we examined the effect of RAF1 on ARL4C expression in AM-1 cells. Raf1 kinase inhibitor I suppressed ERK1/2 activation and ARL4C expression (Figure 2B and supplementary material, Figure S1D). Treatment with SB590885 further reduced ARL4C expression, which was partially decreased by treatment with low concentrations of Raf1 kinase inhibitor I (supplementary material, Figure S1E). The results were consistent with the findings that BRAFV600E activates RAF1 kinase activity [33]. Furthermore, RAF1 knockdown decreased ARL4C expression (Figure 2C and supplementary material, Figure S1C). RAF1 expression in AM-1 cells was higher than that in HeLaS3, A549, SAS or NCI-H520 cells (Figure 2D). Immunohistochemically, RAF1 expression in ameloblastoma was higher than that in adjacent oral non-tumour stratified squamous cell regions (Figure 2E), suggesting that ARL4C expression may depend on the RAF1–MEK/ERK pathway in AM-1 cells. Additionally, early growth response 1 (*EGR1*), FOS-like 1, AP-1 transcription factor subunit (*FOSL1*), cyclin D1 (*CCND1*), and MYC proto-oncogene, bHLH transcription factor [*C-Myc* (*MYC*)] were downregulated by treatment with PD184161 or Raf1 kinase inhibitor I (supplementary material, Figure S1F). However, the *CCND1* and *C-Myc* levels were not regulated by treatment with SB590885, indicating that *CCND1* and *C-Myc*, as well as ARL4C, were not downstream of the BRAFV600E-dependent MEK/ERK pathway.

Next, we assessed the ARL4C expression patterns with BRAFV600E and/or RAF1 in ameloblastoma specimens. Immunohistochemistry revealed that BRAFV600E expression was detected in 25 (65.8%) of 38 tumour lesions but not in non-tumour regions, consistent with previous reports [6,8,9,35] (Figure 2F and Table 2). ARL4C was detected along with the expression of BRAFV600E in 19 of 38 (50%) (Table 2). However, RAF1 expression was clearly and frequently detected in the cytoplasm of the tumour cells (31/38; 81.6%) immunohistochemically (Figure 2F and Table 2). ARL4C-positive cases, which were co-expressed with RAF1, numbered 24/38 (63.2%). ARL4C-positive cases, which were co-expressed with both BRAFV600E and RAF1, numbered 19/38 (50%) (Table 2). Importantly, tumours that were double-positive for BRAFV600E and RAF1 were more frequent (19/28; 67.9%), but not significantly, in ARL4C-positive cases than in ARL4C-negative cases (Figure 2F, lower panel). Conversely, only 4/38 (10.5%) ARL4C-positive cases were negative for both RAF1 and BRAFV600E (Table 2). These data suggest that ARL4C expression might be regulated not only by *BRAF*V600E mutations but also by RAF1 expression in ameloblastoma. No association was found between the expression levels of RAF1 or BRAFV600E and the ameloblastoma subtypes or location, size, and recurrence; however, the rates of RAF1 and BRAFV600E positivity were higher in women (RAF1: $p < 0.05$ and BRAFV600E: $p < 0.05$; Fisher's exact test) (supplementary material, Figure S1G and Table S1).

Primary ameloblastoma cells, AB10 cells, and ABSV cells (ABSV cells harbour a *BRAF*V600E mutation), highly expressed *ARL4C* and *RAF1*, and *ARL4C*; this was dependent on the RAF1 pathway in AB10 cells (Figure 2G and supplementary material, Figure S1H). These data indicated that the RAF1–MEK/ERK

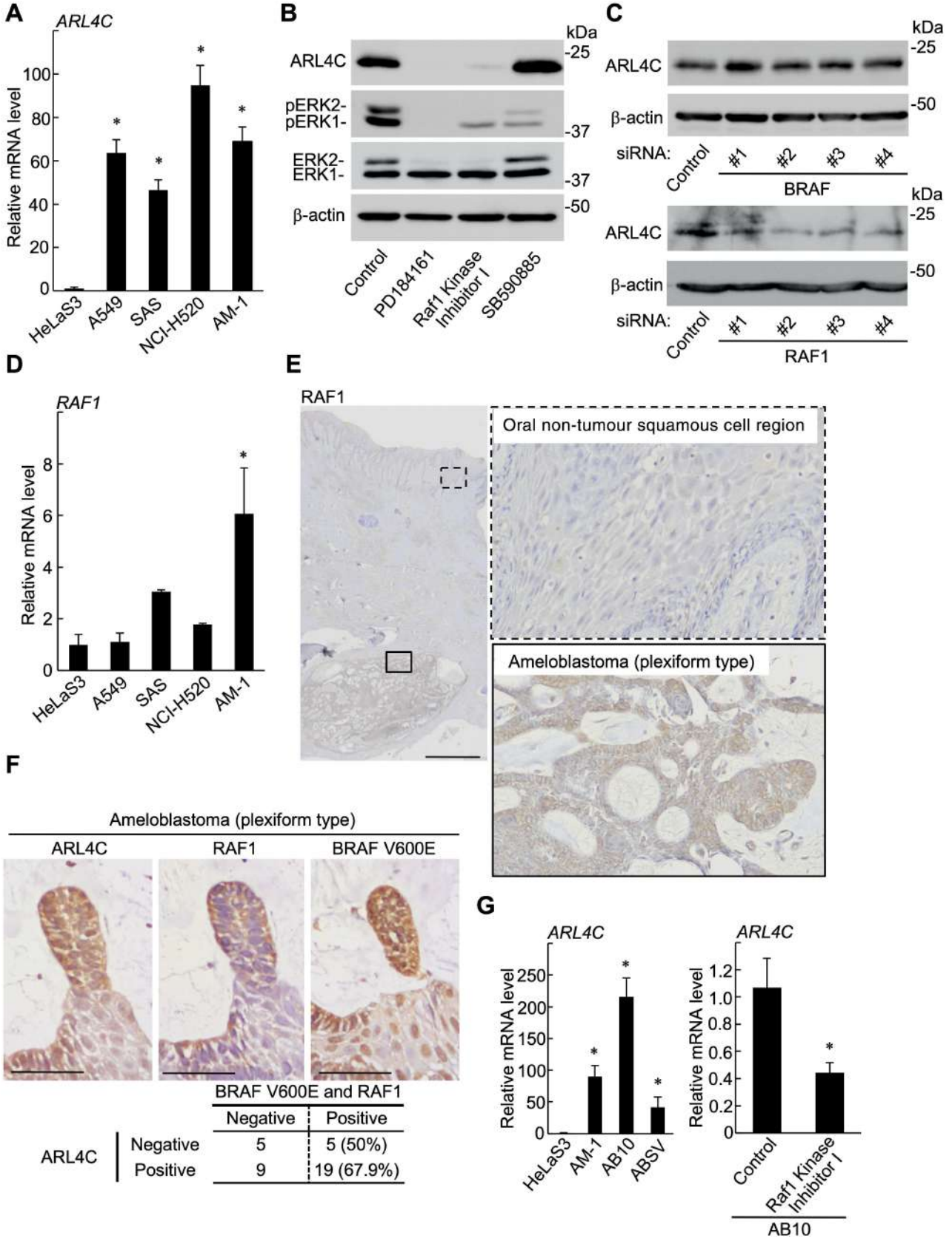

Figure 2 Legend on next page.

Table 2. ARL4C, BRAFV600E, and RAF1 expression in ameloblastomas.

ARL4C	BRAFV600E	RAF1	Number
−	−	−	2
−	−	+	2
−	+	−	1
−	+	+	5
+	−	−	4
+	−	+	5
+	+	−	0
+	+	+	19

−, negative; +, positive.

pathway induces ARL4C expression, not only in immortalized ameloblastoma cells but also in primary ameloblastoma cells.

Loss-of-function experiments using siRNAs and an inhibitor also revealed that RAF1 expression and its activation are involved in AM-1 cell proliferation (Figure 3A). Additionally, SB590885 reduced the cell proliferation capabilities of AM-1 cells (supplementary material, Figure S2A), and simultaneous inhibition combined with Raf1 kinase inhibitor I further suppressed cellular growth (Figure 3B), suggesting that the RAF1–MEK/ERK and BRAFV600E–MEK/ERK pathways might regulate AM-1 cell proliferation independently.

To elucidate the role of RAF1-dependent ARL4C expression in AM-1 cell proliferation, we generated stably ARL4C-expressing cells. Then lentiviral transduction with ARL4C-GFP rescued the Raf1 kinase inhibitor-dependent reduction in ARL4C protein expression and loss-of-function experiment-dependent decreased cellular growth (Figure 3C,D), suggesting that RAF1-dependent ARL4C expression may promote ameloblastoma cell proliferation. Cells expressing ARL4C-GFP showed proliferation capabilities similar to those of control cells expressing GFP (Figure 3C), suggesting that the endogenous ARL4C expression sufficiently regulates the proliferative ability. SB590885 reduced the proliferation capabilities of AM-1 cell expressing not only GFP but also ARL4C-GFP (supplementary material, Figure S2B), supporting the hypothesis that the RAF1–MEK/ERK–ARL4C and BRAFV600E–MEK/ERK pathways might regulate AM-1 cell proliferation independently.

ARL4C expression is involved in the proliferation and migration of ameloblastoma cells

ARL4C expression was shown to be involved in the proliferation and migration of colon cancer, lung cancer, and tongue cancer cells [15,16]. To elucidate the functions of ARL4C in AM-1 cells, ARL4C was knocked down by two different siRNAs (supplementary material, Figure S3A). ARL4C knockdown decreased the migration capability of AM-1 cells (supplementary material, Figure S3B). Because we used ARL4C #1 siRNA, which targets the 3'-UTR (untranslated region) (see supplementary material, Table S2), it did not decrease the amount of exogenously expressed ARL4C-GFP in the cells (supplementary material, Figure S3C). Subsequent ARL4C-GFP expression rescued the ARL4C-knockdown phenotype of tumour cells, excluding siRNA off-target effects (supplementary material, Figure S3D).

To further examine the effect of ARL4C on cell proliferation, ARL4C-knockout AM-1 cells were generated using a CRISPR/Cas9 system (supplementary material, Figure S4A). Genomic deletion and the complete loss of ARL4C protein in the knockout cells were confirmed (Figure 4A and supplementary material, Figure S4B). ARL4C knockout suppressed the proliferation and migration capabilities of AM-1 cells (Figure 4B and supplementary material, Figure S4C). As the ARNO–ARF6 pathway can act downstream of ARL4C to regulate tube formation in intestinal epithelial cells [14] and gene expression in hepatocellular carcinoma [17], we examined whether this pathway could affect the growth potential of AM-1 cells. Treatment with SecinH3 (an inhibitor of ARNO) reduced the cell proliferation capabilities of AM-1 cells (Figure 4C), and its simultaneous inhibition in combination with SB590885 further suppressed cellular growth (Figure 4D). Furthermore, $ARF6^{Q67L}$ (an active ARF6 mutant) [36] rescued ARL4C-

Figure 2. ARL4C expression depends on the RAF1–MEK/ERK pathway in ameloblastoma. (A) *ARL4C* mRNA levels in HeLaS3, A549, SAS, NCI-H520, and AM-1 cells were measured by RT-qPCR. Relative levels of *ARL4C* mRNA expression normalized to *GAPDH* were expressed as fold-change compared with expression in HeLaS3 cells. (B) AM-1 cells were cultured without or with 10 μM PD184161, 10 μM Raf1 kinase inhibitor I or 10 μM SB590885 for 24 h. Cell lysates were probed with anti-ARL4C, anti-phospho-ERK1/2, anti-ERK1/2, and anti-β-actin antibodies. (C) AM-1 cells were transfected with control or four independent BRAF or RAF1 siRNAs. Cell lysates were probed with anti-ARL4C and anti-β-actin antibodies. (D) *RAF1* mRNA levels in HeLaS3, A549, SAS, NCI-H520, and AM-1 cells were measured using RT-qPCR. Relative levels of *RAF1* mRNA expression normalized to *GAPDH* were expressed as fold-change compared with expression in HeLaS3 cells. (E) Representative ameloblastoma tissue stained with anti-RAF1 antibody and haematoxylin. The dashed box and the solid box indicate enlarged images of oral non-tumour squamous cell region and ameloblastoma (plexiform type), respectively. (F) Ameloblastoma tissues ($n = 38$) were stained with anti-ARL4C, anti-RAF1, and BRAFV600E antibodies, and haematoxylin. The numbers of cases that were ARL4C-negative or ARL4C-positive, and BRAFV600E- and RAF1-negative or BRAFV600E- and RAF1-positive are shown below. (G) *ARL4C* mRNA levels in HeLaS3, AM-1, AB10, and ABSV cells were measured using RT-qPCR. Relative levels of *ARL4C* mRNA expression normalized to *GAPDH* were expressed as fold-change compared with expression in HeLaS3 cells (left panel). AB10 cells were cultured without or with 10 μM Raf1 kinase inhibitor I for 24 h. *ARL4C* mRNA levels in AB10 were measured using RT-qPCR. Relative *ARL4C* mRNA levels normalized to *GAPDH* were expressed as fold-change compared with levels in control cells (right panel). Scale bars: 1 mm (E); 40 μm (F). Results are shown as means ± SD of three independent experiments. *$p < 0.01$.

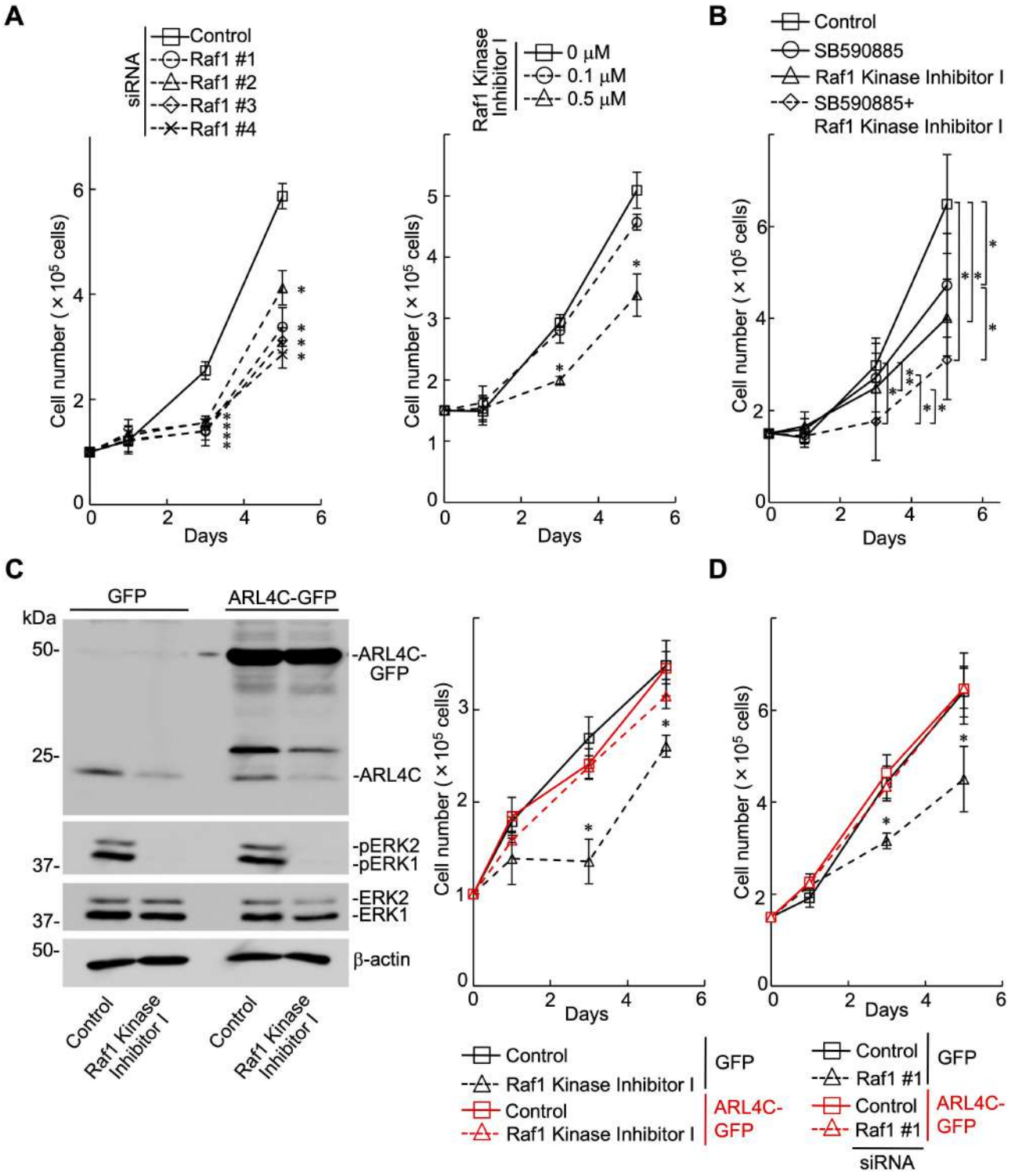

Figure 3. RAF1-dependent ARL4C expression is required for the proliferation of ameloblastoma cells. (A) AM-1 cells were transfected with control or four different RAF1 siRNAs. The cells were cultured for the indicated numbers of days, and cell numbers were counted (left panel). AM-1 cells were cultured without or with 0.1 and 0.5 μM Raf1 kinase inhibitor I for the indicated numbers of days, and cell numbers were counted (right panel). (B) AM-1 cells were cultured without or with 0.5 μM Raf1 kinase inhibitor I and/or 5 μM SB590885 for the indicated numbers of days, and cell numbers were counted. (C) AM-1 cells expressing GFP or ARL4C-GFP were cultured without or with 1 μM Raf1 kinase inhibitor I for 24 h. Cell lysates were probed with anti-ARL4C, anti-phospho-ERK1/2, anti-ERK1/2, and anti-β-actin antibodies (left panels). AM-1 cells expressing GFP or ARL4C-GFP were cultured without or with 0.5 μM Raf1 kinase inhibitor I for the indicated numbers of days, and cell numbers were counted (right panel). (D) AM-1 cells expressing GFP or ARL4C-GFP were transfected with control or RAF1 #1 siRNA. The cells were cultured for the indicated numbers of days, and cell numbers were counted. Results are shown as means ± SD of three independent experiments. *$p < 0.01$; **$p < 0.05$.

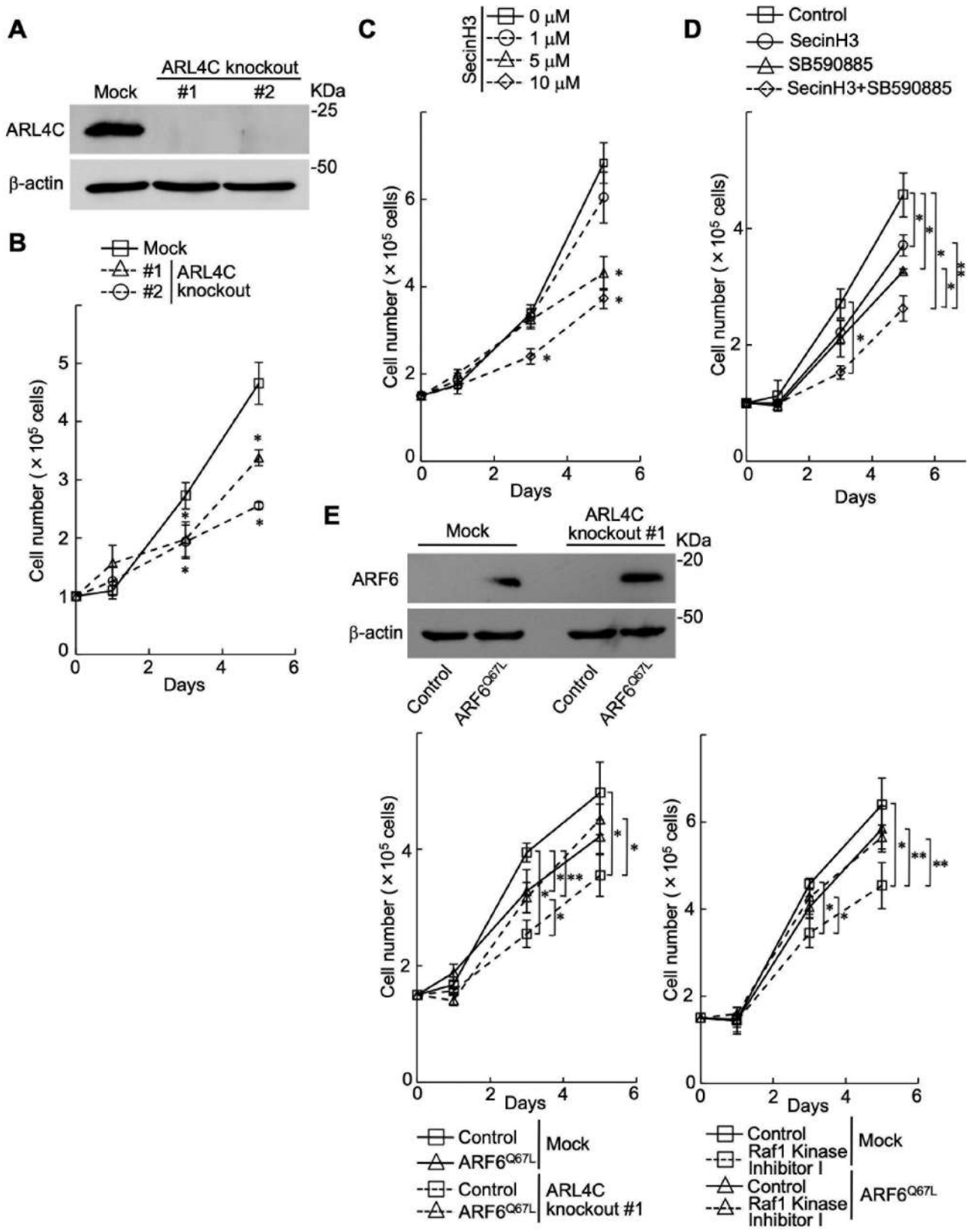

Figure 4. ARL4C expression is involved in the proliferation of ameloblastoma cells. (A) Lysates of ARL4C-knockout AM-1 cells were generated and cell lysates were probed with anti-ARL4C and anti-β-actin antibodies. (B) ARL4C control or knockout AM-1 cells were cultured for the indicated numbers of days, and cell numbers were counted. (C) AM-1 cells were cultured without or with 1, 5, and 10 μM SecinH3 for the indicated numbers of days, and cell numbers were counted. (D) AM-1 cells were cultured without or with 5 μM SecinH3 and/or 5 μM SB590885 for the indicated numbers of days, and cell numbers were counted. (E) ARL4C control or knockout AM-1 cells were transfected with mock or $ARF6^{Q67L}$, and cell lysates were probed with anti-ARF6 and anti-β-actin antibodies (upper panels). ARL4C control or knockout AM-1 cells expressing mock or $ARF6^{Q67L}$ were cultured for the indicated numbers of days, and cell numbers were counted (lower left panel). AM-1 cells expressing mock or $ARF6^{Q67L}$ were cultured without or with 0.5 μM Raf1 kinase inhibitor I for the indicated numbers of days, and cell numbers were counted (lower right panel). Results are shown as means ± SD of three independent experiments. *$p < 0.01$; **$p < 0.05$.

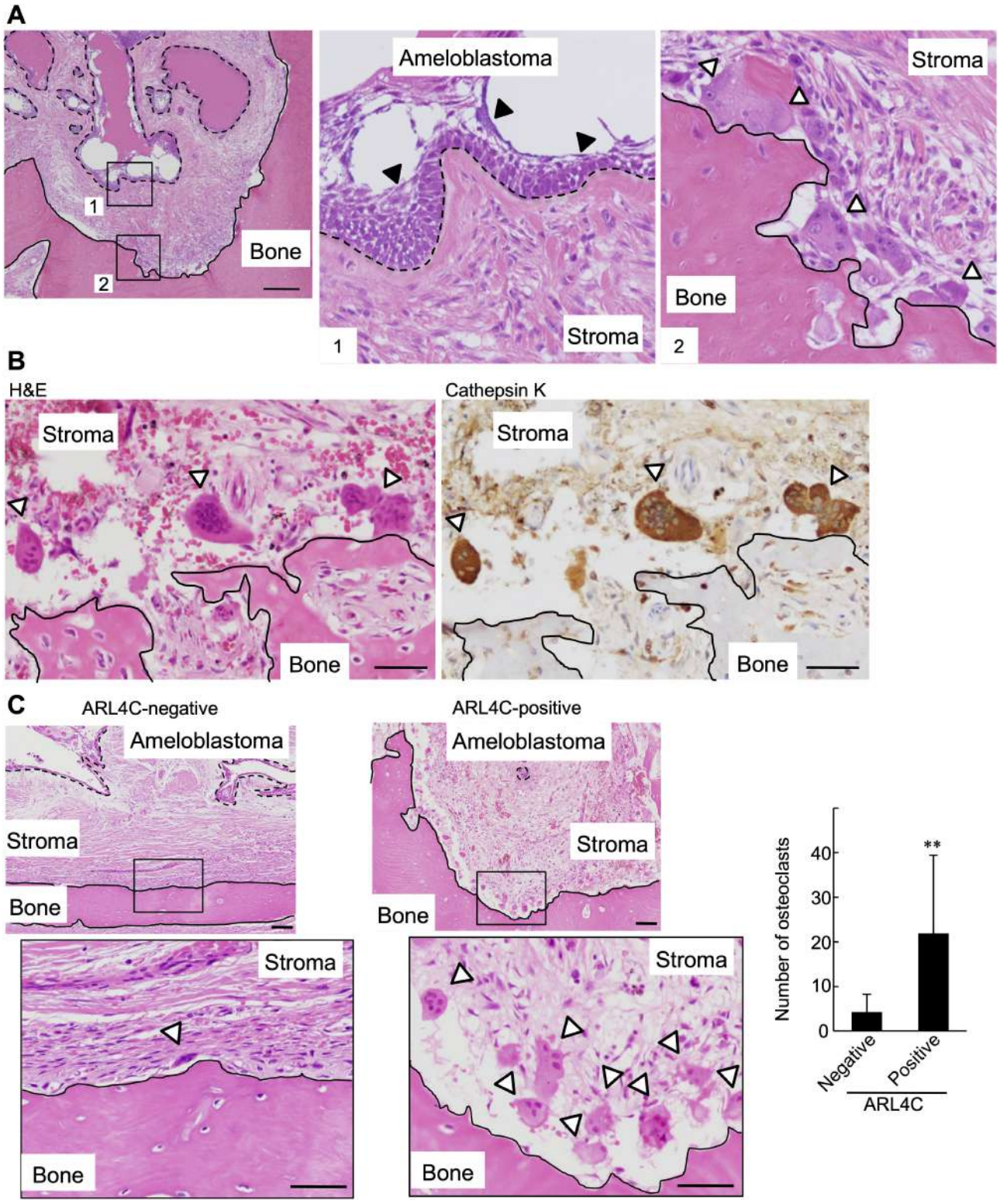

Figure 5. ARL4C expression in ameloblastoma induces osteoclast formation in the ameloblastoma tissues. (A) Ameloblastoma tissues, which were intraosseous, were stained with H&E. Boxes show enlarged images. Black arrowheads and white arrowheads indicate ameloblastoma cells and multinucleated cells, respectively. Dotted lines and black lines indicate the border between ameloblastoma and stroma, and between bone and stroma, respectively. (B) Ameloblastoma tissues, which were intraosseous, were stained with anti-cathepsin K antibody and haematoxylin. White arrowheads indicate multinucleated cells. Black lines indicate the border between bone and stroma. (C) Representative osteoclasts were shown in the ARL4C-negative and ARL4C-positive specimens. The number of osteoclasts was counted in the ARL4C-negative and ARL4C-positive specimens ($n = 22$). White arrowheads indicate osteoclasts. Boxes indicate enlarged images. Dotted lines and black lines indicate the border between ameloblastoma and stroma, and between bone and stroma, respectively. Scale bars: 200 μm (A); 50 μm (B, C). $^{**}p < 0.05$.

knockout- and/or Raf1 kinase inhibitor I-dependent decreased cellular growth (Figure 4E), suggesting that RAF1–MEK/ERK–ARL4C–ARNO–ARF6 signalling might be involved in AM-1 cell proliferation.

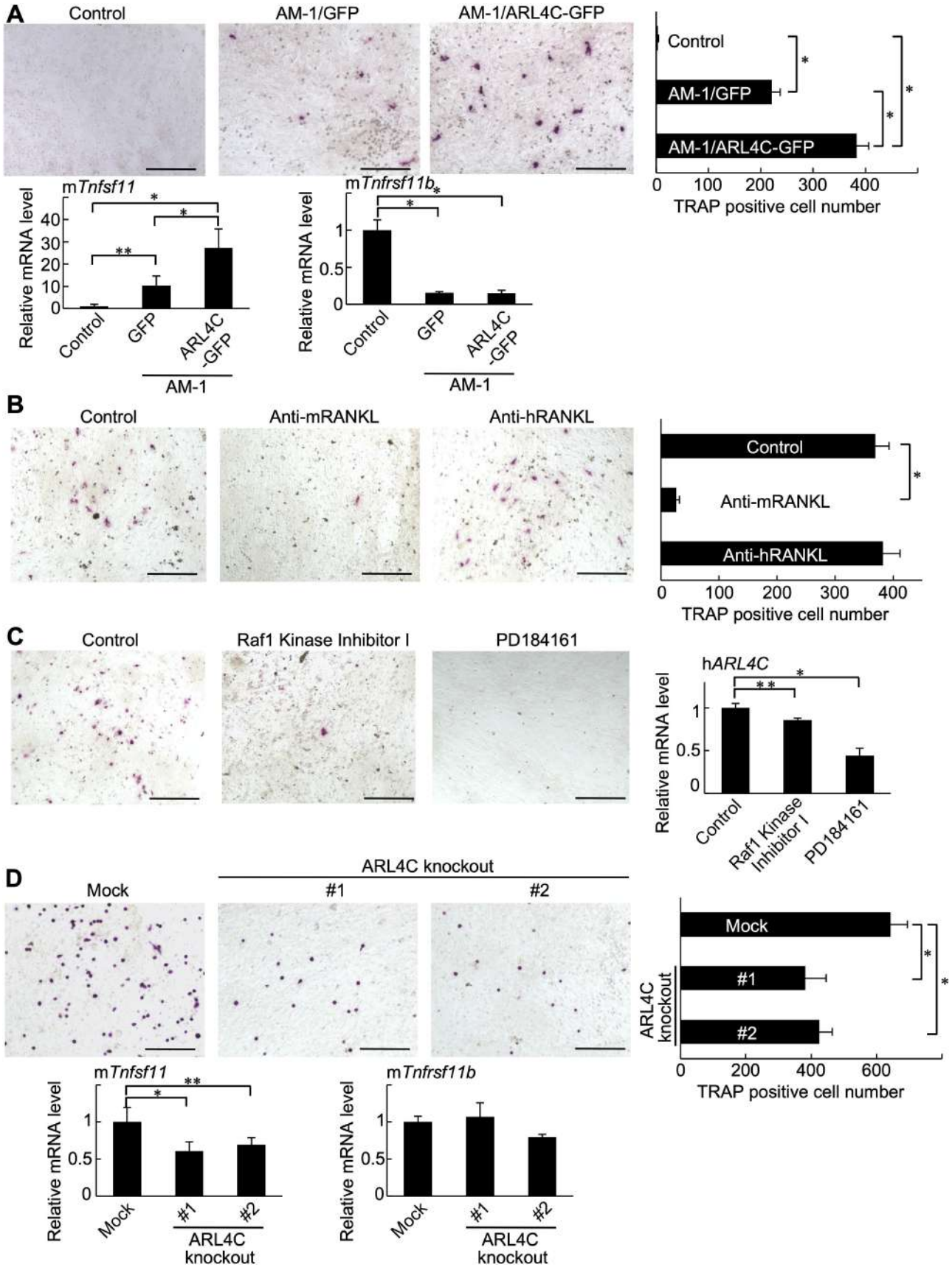

Figure 6 Legend on next page.

ARL4C expression in ameloblastoma induces osteoclast formation

Patients with ameloblastoma often exhibit extensive jaw resorption, which is a common clinical problem. Osteoclasts, multinucleated cells (MNCs) that show TRAP activity, are responsible for bone resorption [37,38]. Therefore, we examined whether or not ARL4C expression in ameloblastoma might induce osteoclast formation. H&E-stained ameloblastoma sections showed that numerous MNCs were aligned on the surface of resorbed bone (Figure 5A and supplementary material, Figure S5). Immunohistochemically, MNCs were positive for cathepsin K (Figure 5B), indicating that the MNCs in the sections are osteoclasts [39]. In our cases ($n = 28$), ameloblastoma cells expressing ARL4C appeared to be separated from osteoclasts at a distance of 678.13 ± 51.49 μm (Figure 5A and supplementary material, Figure S5), suggesting that ameloblastoma may induce osteoclast formation indirectly. The number of osteoclasts in the ARL4C-positive section was more than that in the ARL4C-negative section, suggesting that ARL4C expression may affect osteoclast formation in ameloblastoma (Figure 5C).

To evaluate the involvement of ameloblastoma in osteoclast formation, AM-1 cells expressing GFP or ARL4C-GFP were co-cultured with mouse BMCs and POBs; thus, a few TRAP-positive MNCs and many TRAP-positive mononuclear cells were observed (Figure 6A). However, while MNCs and resorption pits on the Osteo Assay Plate were indeed observed (supplementary material, Figure S6A,B), co-culture with Keratinocyte SFM medium for AM-1 cells greatly suppressed the number and the size of MNCs compared with the culture with only α-MEM medium (data not shown). Here, TRAP-positive cells were counted as osteoclast-like cells. Then AM-1 cells induced TRAP-positive cells, and ARL4C expression further increased the number of TRAP-positive cells (Figure 6A).

Several factors, such as the receptor activator of the NF-κB ligand (RANKL; *Tnfsf11*), its receptor (RANK; *Tnfrsf11a*), and its decoy receptor osteoprotegerin (OPG; *Tnfrsf11b*), are reportedly required for osteoclastogenesis [38,40]. Because the RANKL/RANK pathway regulates osteoclast differentiation, balanced expression of RANKL and OPG is considered critical for regulating osteoclast function. AM-1 cells dramatically induced mouse *Tnfs11* expression and reduced mouse *Tnfsf11b* expression in mouse BMCs and/or POBs when mouse-specific primers were used (Figure 6A, lower panels). ARL4C expression further upregulated the mouse *Tnfsf11* mRNA levels (Figure 6A, lower panels). The *TNFSF11* and *TNFRSF1B* expression in AM-1 cells was comparable to that in HeLaS3, A549, SAS, and NCI-H520 cells (supplementary material, Figure S6C). ARL4C expression slightly, but significantly, upregulated human *TNFSF11* mRNA expression in human AM-1 cells when human-specific primers were used (supplementary material, Figure S6D). However, a few TRAP-positive cells were observed in the co-culture with BMCs and AM-1 cells expressing ARL4C-GFP in the absence of POBs (data not shown), indicating that the amount of RANKL expressed by AM-1 cells might not be sufficient to induce osteoclastogenesis directly. In the co-culture with BMCs, POBs, and AM-1 cells expressing ARL4C-GFP, neutralizing antibodies specific to mouse RANKL, but not human RANKL, reduced the number of TRAP-positive cells (Figure 6B). Therefore, the RANKL expression of POBs induced by AM-1 cells expressing ARL4C-GFP may lead to upregulation of osteoclast formation. Treatment with Raf1 kinase inhibitor I or PD184161 suppressed *ARL4C* expression in AM-1 and the number of TRAP-positive cells (Figure 6C and supplementary material, Figure S6E). Finally, ARL4C-knockout AM-1 cells reduced the number of TRAP-positive cells and mouse *Tnfs11* mRNA expression (Figure 6D). Collectively, these results indicated that ameloblastoma cells indirectly promoted osteoclast formation by regulating the balance of RANKL and OPG in osteoblasts/stromal cells, and that the RAF1–MEK/ERK-dependent expression of ARL4C might be involved in the regulation of this balance.

Discussion

Recent studies have highlighted various gene mutations related to the MAPK pathway, including *FGFR2*, *BRAF*, *KRAS*, *NRAS*, and *HRAS*, in ameloblastoma, with *BRAF*V600E being the most common (40–60%)

Figure 6. ARL4C expression in ameloblastoma induces osteoclast formation indirectly. (A) AM-1 cells (2×10^4 cells) and mouse BMCs (2×10^6 cells) were co-cultured with POBs (1×10^4 cells) for 7 days in 48-well plates. After culture, cells were fixed and stained for TRAP (upper left panels), and TRAP-positive cells were counted (upper right panel). Mouse *Tnfsf11* or *Tnfrsf11b* mRNA levels were measured using RT-qPCR. Relative mouse *Tnfsf11* or *Tnfrsf11b* mRNA levels were normalized to *Gapdh* and expressed as fold-change compared with levels in control cells (lower panels). (B) AM-1 cells and mouse BMCs were co-cultured with POBs without or with neutralizing antibodies to mouse RANKL (10 ng/ml) or human RANKL (10 ng/ml) for 7 days in 48-well plates. After culture, cells were fixed and stained for TRAP (left panels), and TRAP-positive cells were counted (right panel). (C) AM-1 cells and mouse BMCs were co-cultured with POBs without or with10 μM Raf1 kinase inhibitor I or 10 μM PD184161 initially for 2 days and cultured for a total of 7 days in 48-well plates. After culture, cells were fixed and stained for TRAP (left panels). Human *ARL4C* mRNA levels were measured using RT-qPCR. Relative *ARL4C* mRNA levels normalized to *GAPDH* were expressed as fold-change compared with levels in control cells (right panel). (D) ARL4C-knockout AM-1 cells and mouse BMCs were co-cultured with POBs for 7 days in 48-well plates. After culture, cells were fixed and stained for TRAP (upper left panels), and TRAP-positive cells were counted (upper right panel). Mouse *Tnfsf11* or *Tnfrsf11b* mRNA levels were measured using RT-qPCR. Relative mouse *Tnfsf11* or *Tnfrsf11b* mRNA levels normalized to *Gapdh* were expressed as fold-change compared with levels in control cells (lower panels). Results are shown as means ± SD of three independent experiments. Scale bars: 200 μm. $^*p < 0.01$; $^{**}p < 0.05$.

[6,8,9,35], suggesting that *BRAF*V600E mutations may be involved in the aetiology of ameloblastoma development.

Consistently, our immunohistochemical analyses demonstrated that the expression of BRAFV600E, which coincided 100% with the molecular detection of *BRAF*V600E mutations [8], was observed in 25 (65.8%) of 38 cases. *BRAF*V600E mutations are present in numerous malignant tumours, including melanoma, hairy cell leukaemia, papillary thyroid carcinoma, and colorectal cancer [34,41–44], and these mutations induce MEK/ERK activation, which is involved in tumourigenesis [45]. Previously, a heterozygous *BRAF*V600E mutation was detected in ameloblastoma specimens and cell lines [6,8,9,35]. Therefore, *BRAF*V600E mutations in ameloblastoma might be associated with lower oncogenic potential compared with malignant tumours harbouring homozygous mutations. Notably, BRAFV600E positivity accompanied by ARL4C and RAF1 negativity was seen in only 1 of 38 cases (2.6%) (see Table 2), suggesting that *BRAF*V600E mutations alone may not be sufficient to induce ameloblastoma. Similarly, *BRAF*V600E mutations were observed in 39 (89%) of 44 human cases of benign naevi, indicating that BRAF activation alone is not sufficient for the development of melanoma [46]. Another molecular mechanism besides heterozygous *BRAF*V600E mutation may be involved in the development of ameloblastoma.

ARL4C was highly expressed with RAF1 and BRAFV600E in the lesional tissue of ameloblastoma specimens. The RAF1–MEK/ERK and BRAFV600E–MEK/ERK pathways may cooperatively induce the expression of ARL4C in ameloblastoma. The current loss-of-function experiments using inhibitors or siRNAs demonstrated that the RAF1–MEK/ERK–ARL4C–ARNO–ARF6 pathway and the BRAFV600E–MEK/ERK pathway independently promote AM-1 cell proliferation. Collectively, these results support the idea that their combined signal inhibition may be an effective anti-tumour therapeutic strategy for patients with ameloblastoma. ARL4C reportedly contributes to oncogenesis through its overexpression by multiple mechanisms in a cell-context-dependent manner [15–17]. In ameloblastoma cells, ARL4C expression was shown to depend on the RAF1–MEK/ERK pathway (see Figure 2B), suggesting that the RAF1–MEK/ERK pathway may be activated in ameloblastoma.

The overexpression of RAF1 has been observed in various cancers, such as lung adenocarcinomas and multiple myeloma [47,48], suggesting that its overexpression may be associated with tumourigenesis. RAF1 expression was clearly elevated in ameloblastoma cell lines and specimens (see Figure 2D,E). Cancer samples bearing *BRAF*V600E mutants did not contain *RAS* mutations [34,43], indicating their exclusive relationship. However, wild-type BRAF forms a complex with RAF1 and then increases RAF1 kinase activity, thereby stimulating the MEK/ERK pathway [33]. Although the definitive mechanisms by which the BRAFV600E–MEK/ERK pathway alone did not affect the expression of ARL4C remain unclear, two hypotheses are proposed. First, so-called paradoxical MAPK activation due to BRAF inhibitor-mediated homodimerization and heterodimerization of wild-type BRAF or RAF1 [49] leads to the secondary activation of the RAF1–MEK/ERK pathway, thereby maintaining ARL4C expression. Second, the contribution of BRAFV600E to MEK–ERK pathway activation may be relatively low. Thus, it is possible that BRAFV600E is not sufficient to induce ARL4C expression in the presence of RAF1 overexpression, because the complex formation of BRAFV600E and RAF1 inhibits the kinase activity of BRAFV600E and ERK activation [50]. It is therefore intriguing to speculate that cooperative activation of BRAFV600E and RAF1 would be the aetiology of ameloblastoma cell proliferation and that such cooperative activation might induce the clinical aggressiveness of ameloblastoma beyond the category with benign neoplasia.

While some reports have shown that RANKL, which is secreted by ameloblastoma cells, induces osteoclastogenesis [51,52], ameloblastoma cells appeared to be located separately from osteoclasts in ameloblastoma specimens. We thus hypothesized that ameloblastoma cells induce osteoclast formation indirectly. In support of this, the role of stromal cells has been emphasized in the osteoclastogenesis of patients with ameloblastoma [53]. In the current co-culture system, ameloblastoma cells induced *Tnfsf11* expression and reduced *Tnfrsf11b* expression in mouse BMCs and/or POBs, indicating that the interaction of tumour cells and stromal cells/osteoblasts plays a pivotal role in ameloblastoma mediated-osteoclast formation. Although the precise mechanism underlying the upregulation of RANKL or the mechanism of OPG downregulation by AM-1 was unclear, our findings were consistent with previous findings that oral squamous cells induced osteoclast formation by increasing the RANK/OPG ratio of osteoblasts/stromal cells through interaction with osteoblasts/stromal cells [31].

In summary, we found that ARL4C is highly expressed in ameloblastoma specimens with high frequencies and in ameloblastoma cell lines. We also demonstrated that the RAF1–MEK/ERK pathway induces ARL4C expression to regulate ameloblastoma cellular growth positively and promote ameloblastoma-mediated osteoclast formation (supplementary material, Figure S6F). Therefore, these results suggest that the RAF1–MEK/ERK–ARL4C axis contributes to the development of ameloblastoma.

Acknowledgements

We thank Drs K Nagata, T Harada, Y Kami, H Hiura, Y Tajiri, K Hasegawa, R Nagano, S Nakamura, Y Mori, and H Wada for valuable technical support in this research. We also thank the Research Support Center, Graduate School of Medical Sciences, Kyushu University. We appreciate the technical assistance from The

Joint Use Laboratories, Faculty of Dental Science, Kyushu University. This work was supported by JSPS KAKENHI grants to SF (2020–2022) (20K09906) and TK (2020–2022) (20K10096), Fukuoka Foundation for Sound Health Cancer Research Fund, Takeda Science Foundation, The Shin-Nihon Foundation of Advanced Medical Research, and SGH Foundation (to SF), and Maritza ja Reino Salonen Foundation (to KH).

Author contributions statement

SF carried out experiments and conceived and wrote the manuscript. TI carried out immunohistochemistry experiments and co-wrote the manuscript. MK carried out ARL4C expression experiments and clinicopathological analyses. TF and SS analysed the immunohistochemical data. SM and AK interpreted the data and co-wrote the manuscript. EJ carried out osteoclast formation experiments. KK, JP, JC, PM, and KH established primary ameloblastoma cells and interpreted the data. TK carried out data interpretation and co-wrote the manuscript. All authors were involved in writing the paper and had final approval of the submitted and published versions.

References

1. Vered M, Muller S, Heikinhemio K. Ameloblastoma. Benign epithelial odontogenic tumours. In *WHO Classification of Head and Neck Tumours* (4th edn), El-Naggar AK, Chan JKC, Grandis JR, *et al*. (eds). IARC: Lyon, 2017; 215–218.
2. Mendenhall WM, Werning JW, Fernandes R, *et al*. Ameloblastoma. *Am J Clin Oncol* 2007; **30:** 645–648.
3. Heikinheimo K, Huhtala JM, Thiel A, *et al*. The mutational profile of unicystic ameloblastoma. *J Dent Res* 2019; **98:** 54–60.
4. Mano H. Cancer genomic medicine in Japan. *Proc Jpn Acad Ser B Phys Biol Sci* 2020; **96:** 316–321.
5. Buchner A, Merrell PW, Carpenter WM. Relative frequency of central odontogenic tumors: a study of 1,088 cases from Northern California and comparison to studies from other parts of the world. *J Oral Maxillofac Surg* 2006; **64:** 1343–1352.
6. Kurppa KJ, Catón J, Morgan PR, *et al*. High frequency of BRAF V600E mutations in ameloblastoma. *J Pathol* 2014; **232:** 492–498.
7. Sweeney RT, McClary AC, Myers BR, *et al*. Identification of recurrent *SMO* and *BRAF* mutations in ameloblastomas. *Nat Genet* 2014; **46:** 722–725.
8. Brown NA, Rolland D, McHugh JB, *et al*. Activating *FGFR2–RAS–BRAF* mutations in ameloblastoma. *Clin Cancer Res* 2014; **20:** 5517–5526.
9. Seki-Soda M, Sano T, Ito K, *et al*. An immunohistochemical and genetic study of $BRAF^{V600E}$ mutation in Japanese patients with ameloblastoma. *Pathol Int* 2020; **70:** 224–230.
10. Tan S, Pollack JR, Kaplan MJ, *et al*. *BRAF* inhibitor treatment of primary *BRAF*-mutant ameloblastoma with pathologic assessment of response. *Oral Surg Oral Med Oral Pathol Oral Radiol* 2016; **122:** e5–e7.
11. Faden DL, Algazi A. Durable treatment of ameloblastoma with single agent BRAFi Re: clinical and radiographic response with combined BRAF-targeted therapy in stage 4 ameloblastoma. *J Natl Cancer Inst* 2016; **109:** djw190.
12. Fernandes GS, Girardi DM, Bernardes JPG, *et al*. Clinical benefit and radiological response with BRAF inhibitor in a patient with recurrent ameloblastoma harboring V600E mutation. *BMC Cancer* 2018; **18:** 887.
13. Matsumoto S, Fujii S, Kikuchi A. Arl4c is a key regulator of tubulogenesis and tumourigenesis as a target gene of Wnt–β-catenin and growth factor–Ras signalling. *J Biochem* 2017; **161:** 27–35.
14. Matsumoto S, Fujii S, Sato A, *et al*. A combination of Wnt and growth factor signaling induces Arl4c expression to form epithelial tubular structures. *EMBO J* 2014; **33:** 702–718.
15. Fujii S, Matsumoto S, Nojima S, *et al*. Arl4c expression in colorectal and lung cancers promotes tumorigenesis and may represent a novel therapeutic target. *Oncogene* 2015; **34:** 4834–4844.
16. Fujii S, Shinjo K, Matsumoto S, *et al*. Epigenetic upregulation of ARL4C, due to DNA hypomethylation in the 3′-untranslated region, promotes tumorigenesis of lung squamous cell carcinoma. *Oncotarget* 2016; **7:** 81571–81587.
17. Harada T, Matsumoto S, Hirota S, *et al*. Chemically modified antisense oligonucleotide against ARL4C inhibits primary and metastatic liver tumor growth. *Mol Cancer Ther* 2019; **18:** 602–612.
18. Kimura K, Matsumoto S, Harada T, *et al*. ARL4C is associated with initiation and progression of lung adenocarcinoma and represents a therapeutic target. *Cancer Sci* 2020; **111:** 951–961.
19. Hu Q, Masuda T, Sato K, *et al*. Identification of *ARL4C* as a peritoneal dissemination-associated gene and its clinical significance in gastric cancer. *Ann Surg Oncol* 2018; **25:** 745–753.
20. Isono T, Chano T, Yoshida T, *et al*. ADP-ribosylation factor-like 4C is a predictive biomarker of poor prognosis in patients with renal cell carcinoma. *Am J Cancer Res* 2019; **9:** 415–423.
21. Wakinoue S, Chano T, Amano T, *et al*. ADP-ribosylation factor-like 4C predicts worse prognosis in endometriosis-associated ovarian cancers. *Cancer Biomark* 2019; **24:** 223–229.
22. Chen Q, Weng HY, Tang XP, *et al*. ARL4C stabilized by AKT/-mTOR pathway promotes the invasion of PTEN-deficient primary human glioblastoma. *J Pathol* 2019; **247:** 266–278.
23. Matsumoto S, Kurimoto T, Taketo MM, *et al*. The WNT/MYB pathway suppresses KIT expression to control the timing of salivary proacinar differentiation and duct formation. *Development* 2016; **143:** 2311–2324.
24. Mikami Y, Fujii S, Kohashi KI, *et al*. Low-grade myofibroblastic sarcoma arising in the tip of the tongue with intravascular invasion: a case report. *Oncol Lett* 2018; **16:** 3889–3894.
25. Harada H, Mitsuyasu T, Nakamura N, *et al*. Establishment of ameloblastoma cell line, AM-1. *J Oral Pathol Med* 1998; **27:** 207–212.
26. Miyoshi H, Blömer U, Takahashi M, *et al*. Development of a self-inactivating lentivirus vector. *J Virol* 1998; **72:** 8150–8157.
27. Hasegawa K, Fujii S, Matsumoto S, *et al*. YAP signaling induces PIEZO1 to promote oral squamous cell carcinoma cell proliferation. *J Pathol* 2021; **253:** 80–93.
28. Mikami Y, Fujii S, Nagata K, *et al*. GLI-mediated keratin 17 expression promotes tumor cell growth through the anti-apoptotic function in oral squamous cell carcinomas. *J Cancer Res Clin Oncol* 2017; **143:** 1381–1393.
29. Fujii S, Tajiri Y, Hasegawa K, *et al*. The TRPV4–AKT axis promotes oral squamous cell carcinoma cell proliferation via CaMKII activation. *Lab Invest* 2020; **100:** 311–323.
30. Hsu PD, Scott DA, Weinstein JA, *et al*. DNA targeting specificity of RNA-guided Cas9 nucleases. *Nat Biotechnol* 2013; **31:** 827–832.
31. Tada T, Jimi E, Okamoto M, *et al*. Oral squamous cell carcinoma cells induce osteoclast differentiation by suppression of osteoprotegerin expression in osteoblasts. *Int J Cancer* 2005; **116:** 253–262.
32. Fujii S, Nagata K, Matsumoto S, *et al*. Wnt/β-catenin signaling, which is activated in odontomas, reduces Sema3A expression to regulate odontogenic epithelial cell proliferation and tooth germ development. *Sci Rep* 2019; **9:** 4257.

33. Garnett MJ, Rana S, Paterson H, *et al*. Wild-type and mutant B-RAF activate C-RAF through distinct mechanisms involving heterodimerization. *Mol Cell* 2005; **20:** 963–969.
34. Rajagopalan H, Bardelli A, Lengauer C, *et al*. Tumorigenesis: *RAF/RAS* oncogenes and mismatch-repair status. *Nature* 2002; **418:** 934.
35. Yukimori A, Oikawa Y, Morita KI, *et al*. Genetic basis of calcifying cystic odontogenic tumors. *PLoS One* 2017; **12:** e0180224.
36. Aikawa Y, Martin TF. ARF6 regulates a plasma membrane pool of phosphatidylinositol(4,5)bisphosphate required for regulated exocytosis. *J Cell Biol* 2003; **162:** 647–659.
37. Nakamura I, Takahashi N, Jimi E, *et al*. Regulation of osteoclast function. *Mod Rheumatol* 2012; **22:** 167–177.
38. Takayanagi H. SnapShot: Osteoimmunology. *Cell Metab* 2015; **21:** 502.e1.
39. Tohyama R, Kayamori K, Sato K, *et al*. Establishment of a xenograft model to explore the mechanism of bone destruction by human oral cancers and its application to analysis of role of RANKL. *J Oral Pathol Med* 2016; **45:** 356–364.
40. Boyle WJ, Simonet WS, Lacey DL. Osteoclast differentiation and activation. *Nature* 2003; **423:** 337–342.
41. Curtin JA, Fridlyand J, Kageshita T, *et al*. Distinct sets of genetic alterations in melanoma. *N Engl J Med* 2005; **353:** 2135–2147.
42. Tiacci E, Trifonov V, Schiavoni G, *et al*. *BRAF* mutations in hairy-cell leukemia. *N Engl J Med* 2011; **364:** 2305–2315.
43. Davies H, Bignell GR, Cox C, *et al*. Mutations of the *BRAF* gene in human cancer. *Nature* 2002; **417:** 949–954.
44. Puxeddu E, Moretti S, Elisei R, *et al*. $BRAF^{V599E}$ mutation is the leading genetic event in adult sporadic papillary thyroid carcinomas. *J Clin Endocrinol Metab* 2004; **89:** 2414–2420.
45. Niault TS, Baccarini M. Targets of Raf in tumorigenesis. *Carcinogenesis* 2010; **31:** 1165–1174.
46. Pollock PM, Harper UL, Hansen KS, *et al*. High frequency of *BRAF* mutations in nevi. *Nat Genet* 2003; **33:** 19–20.
47. Cekanova M, Majidy M, Masi T, *et al*. Overexpressed Raf-1 and phosphorylated cyclic adenosine 3′-5′-monophosphatate response element-binding protein are early markers for lung adenocarcinoma. *Cancer* 2007; **109:** 1164–1173.
48. Müller E, Bauer S, Stühmer T, *et al*. Pan-Raf co-operates with PI3K-dependent signalling and critically contributes to myeloma cell survival independently of mutated RAS. *Leukemia* 2017; **31:** 922–933.
49. Poulikakos PI, Zhang C, Bollag G, *et al*. RAF inhibitors transactivate RAF dimers and ERK signalling in cells with wild-type BRAF. *Nature* 2010; **464:** 427–430.
50. Karreth FA, DeNicola GM, Winter SP, *et al*. C-Raf inhibits MAPK activation and transformation by $B\text{-}Raf^{V600E}$. *Mol Cell* 2009; **36:** 477–486.
51. Sandra F, Hendarmin L, Kukita T, *et al*. Ameloblastoma induces osteoclastogenesis: a possible role of ameloblastoma in expanding in the bone. *Oral Oncol* 2005; **41:** 637–644.
52. Tay JY, Bay BH, Yeo JF, *et al*. Identification of RANKL in osteolytic lesions of the facial skeleton. *J Dent Res* 2004; **83:** 349–353.
53. Sathi GS, Nagatsuka H, Tamamura R, *et al*. Stromal cells promote bone invasion by suppressing bone formation in ameloblastoma. *Histopathology* 2008; **53:** 458–467.

SUPPLEMENTARY MATERIAL ONLINE

Supplementary materials and methods

Figure S1. ARL4C expression depends on the RAF1–MEK/ERK pathway in ameloblastoma

Figure S2. The effect of BRAFV600E signalling on the proliferation of ameloblastoma cells

Figure S3. ARL4C expression is involved in the migration of ameloblastoma cells

Figure S4. Generation of ARL4C-knockout cells

Figure S5. ARL4C expression in ameloblastoma tissues

Figure S6. ARL4C expression in ameloblastoma induces osteoclast formation

Table S1. Clinicopathological data of the patients with ameloblastoma

Table S2. The sequences of siRNAs used in this study

Table S3. List of the RT-qPCR primers used in this study